Nanomaterials and Nanotechnology

OPEN ACCESS
ARTICLE

Preparation of [C_{60}]Fullerene Nanowhisker-gold Nanoparticle Composites and Reduction of 4-Nitrophenol through Catalysis

Regular Paper

Jeong Won Ko[1], Jiulong Li[2] and Weon Bae Ko[1,2]*

1 Department of Convergence Science, Graduate School, Sahmyook University, Seoul, South Korea
2 Department of Chemistry, Sahmyook University, Seoul, South Korea
*Corresponding author(s) E-mail: kowb@syu.ac.kr

Received 22 October 2015; Accepted 01 December 2015

DOI: 10.5772/62086

Abstract

A gold nanoparticle solution was prepared by adding sodium borohydride ($NaBH_4$), trisodium citrate dihydrate ($C_6H_5Na_3O_7 \cdot 2H_2O$), cetyltrimethyl ammonium bromide (CTAB,$(C_{16}H_{33})N(CH_3)_3Br$), ascorbic acid ($C_6H_8O_6$), and potassium tetrachloroaurate(III)($KAuCl_4$) to distilled water and stirring the solution for 15 min. [C_{60}]fullerene nanowhisker-gold nanoparticle composites were synthesized using C_{60}-saturated toluene, the gold nanoparticle solution, and isopropyl alcohol by liquid-liquid interfacial precipitation (LLIP).

The product of the nanocomposites was characterized by X-ray diffraction, scanning electron microscopy, Raman spectroscopy, transmission electron microscopy, and solid-state ^{13}C-nuclear magnetic resonance spectroscopy. The catalytic activity of the [C_{60}]fullerene nanowhisker-gold nanoparticle composites was confirmed in 4-nitrophenol reduction by UV-vis spectroscopy.

Keywords [C_{60}]Fullerene Nanowhisker-gold Nanoparticle Composites, Catalyst, 4-nitrophenol, Reduction

1. Introduction

The best known fullerene is C_{60}, which consists of carbon bonded into 12 pentagonal and 20 hexagonal rings [1]. Polymerization of [C_{60}]fullerene can occur by a cycloadditive reaction, which forms a four-membered ring between adjacent [C_{60}]fullerenes [2]. A crystalline fibre of this carbon nanomaterial is called a [C_{60}]fullerene nanowhisker. [C_{60}]fullerene nanowhiskers can act as an n-type semiconducting material, and are used in a wide range of applications, including photocatalysis, chemical sensors, solar cells, field-effect transistors, and electronic devices [2,3].

The liquid-liquid interfacial precipitation (LLIP) method relies on diffusion of a poor fullerene solvent, such as isopropyl alcohol, into a saturated toluene solution of fullerenes [4]. [C_{60}]fullerene nanowhiskers are synthesized using the LLIP method [4], which has been widely applied [5-12]. The [C_{60}]fullerene nanowhiskers show good electrical conductivity [13] and have a large surface area [14, 15]. The growth of [C_{60}]fullerene nanowhiskers is affected by temperature, light, ratio of poor solvent to good solvent during LLIP, and concentration of water [16-20].

[C_{60}]Fullerene nanowhiskers are composed of C_{60} molecules weakly bonded by van der Waals forces [21,22]. After electron beam irradiation, [C_{60}]fullerene nanowhiskers show higher Young's modulus [24] than pristine C_{60} crystals [22], and stronger thermal stability [23]. When Miyazawa et al. used Raman laser-beam irradiation, [C_{60}]fullerene nanowhiskers became polymerized [21,22]. Rao et al. found that the shift of $A_g(2)$ peak was a good indicator for [C_{60}]fullerene nanowhisker polymerization, as the peak $A_g(2)$ pentagonal pinch mode of C_{60} shifted downward, from 1469 cm^{-1} to 1457 cm^{-1} upon photopolymerization [22,25]. Gold nanoparticles have been used for hydrogenation of aromatic nitro compounds because of their higher catalytic efficiency compared to bulk catalysts, which can be attributed to their large surface-to-volume ratio [26]. The dispersion of gold nanoparticles on nanoporous fullerene nanowhiskers is attractive for catalytic applications [27,28]. The reduction of 4-nitrophenol to 4-aminophenol in the presence of $NaBH_4$ with gold nanoparticles is a commercially important intermediate for the manufacture of analgesic and antipyretic drugs [29-32]. Examples of the use of 4-nitrophenol in classical reaction tests to evaluate catalytic properties of various metal nanoparticles, or in similar kinetic studies with gold nanoparticles dispersed in other conducting matrices, are given in the following literature [33-36]. The present authors have investigated the characterization of gold nanoparticles incorporating [C_{60}]fullerene nanowhiskers and their catalytic activity for 4-nitrophenol reduction in the presence of sodium borohydride ($NaBH_4$), as determined by UV-vis spectrophotometry.

2. Experiment

2.1 Reagents and instruments

Sodium borohydride ($NaBH_4$) was purchased from Kanto Chemical Co., Inc., and trisodium citrate dihydrate ($C_6H_5Na_3O_7$ $2H_2O$), cetyltrimethyl ammonium bromide ($(C_{16}H_{33})N(CH_3)_3Br$), and toluene were obtained from Samchun Chemicals. Ascorbic acid ($C_6H_8O_6$) and potassium tetrachloroaurate (III) n-hydrate ($KAuCl_4$ nH_2O) were supplied by Sigma-Aldrich. [C_{60}]fullerene was supplied by Tokyo Chemical Industry Co., Ltd.

X-ray diffraction (XRD; Bruker, D8 Advance) analysis was used to examine the structure of the nanocomposites at 40 kV and 40 mA. Imaging of the sample surface was performed by scanning electron microscopy (SEM; JEOL Ltd., JSM-6510) at an accelerating voltage of 0.5 to 30 kV. The particle size and morphology of the sample were identified by transmission electron microscopy (TEM; AP Tech, Tecnai G2 F30 S-Twin) at an acceleration voltage of 200 kV. Solid-state ^{13}C-CP/MAS nuclear magnetic resonance spectroscopy (Agilent Technologies Korea, DD2 700) was used for observing the chemical shift of carbon in the [C_{60}]fullerene nanowhisker-gold nanoparticle composites. Raman spectroscopy (Thermo Fisher Scientific, DXR Raman Microscope) was used for observing the polymerization of the composites, and UV-vis spectrophotometry (Shimazu UV-1691 PC) was used to characterize their catalytic activity.

2.2 Synthesis of [C_{60}]fullerene nanowhisker-gold nanoparticle composites

2.2.1 Synthesis of gold nanoparticles

A gold nanoparticle seed solution was prepared by dissolving $2.5x10^{-4}$ M potassium tetrachloroaurate (III) ($KAuCl_4$), $2.5x10^{-4}$ M trisodium citrate dihydrate ($C_6H_5Na_3O_7 \bullet 2H_2O$), and 6 ml of 0.1M sodium borohydride ($NaBH_4$) in 5 ml of distilled water. A gold nanoparticle growth solution was prepared with $2.5x10^{-4}$ M $KAuCl_4$ and $2.5x10^{-4}$ M cetyltrimethyl ammonium bromide ($(C_{16}H_{33})N(CH_3)_3Br$) in 20 ml of distilled water. Gold nanoparticles were prepared by mixing 5 ml of seeding solution with 15 ml of growth solution, and then adding 0.1 ml of ascorbic acid ($C_6H_8O_6$) to the solution and stirring for 15 min.

2.2.2 Synthesis of [C_{60}]fullerene nanowhisker-gold nanoparticle composites

40 mg of [C_{60}]fullerene and 40 ml of toluene were added into a 50 ml Erlenmeyer flask, and then stirred for 15 min and ultrasonicated for 45 min. [C_{60}]fullerene solution was dissolved in toluene and the solution was filtered through filter paper. The [C_{60}]fullerene solution and isopropyl alcohol were placed in the refrigerator for 20 min.

2 ml of [C_{60}]fullerene solution, 1 ml of gold nanoparticle solution, and 15 ml of isopropyl alcohol were placed in a 20 ml vial. The mixture solution was ultrasonicated for 10 min, and refrigerated for 24 h. The cold mixed solution was filtered through filter paper, and then dried to the solid state in an oven at 100℃ for 5 h. The amount of gold nanoparticles loaded on the fullerene nanowhiskers was 0.25 mM.

2.2.3 Characterization of [C_{60}]fullerene nanowhisker-gold nanoparticle composites

The XRD pattern of the [C_{60}]fullerene nanowhisker-gold nanoparticle composites was obtained from powder X-ray diffraction with Cu Kα radiation (λ=1.54178 Å). The morphological shape of the nanocomposites was observed by SEM, and TEM was used to observe the specimen size. The composites were characterized using Raman spectroscopy, and analysed by solid-state ^{13}C-CP/MAS nuclear magnetic resonance spectroscopy.

2.2.4 Catalytic activity evaluation through 4-nitrophenol reduction

The absorbance peak in the UV-vis spectrum of 1.5 mg (1.1 mM) 4-nitrophenol at 400 nm was monitored, as it ap-

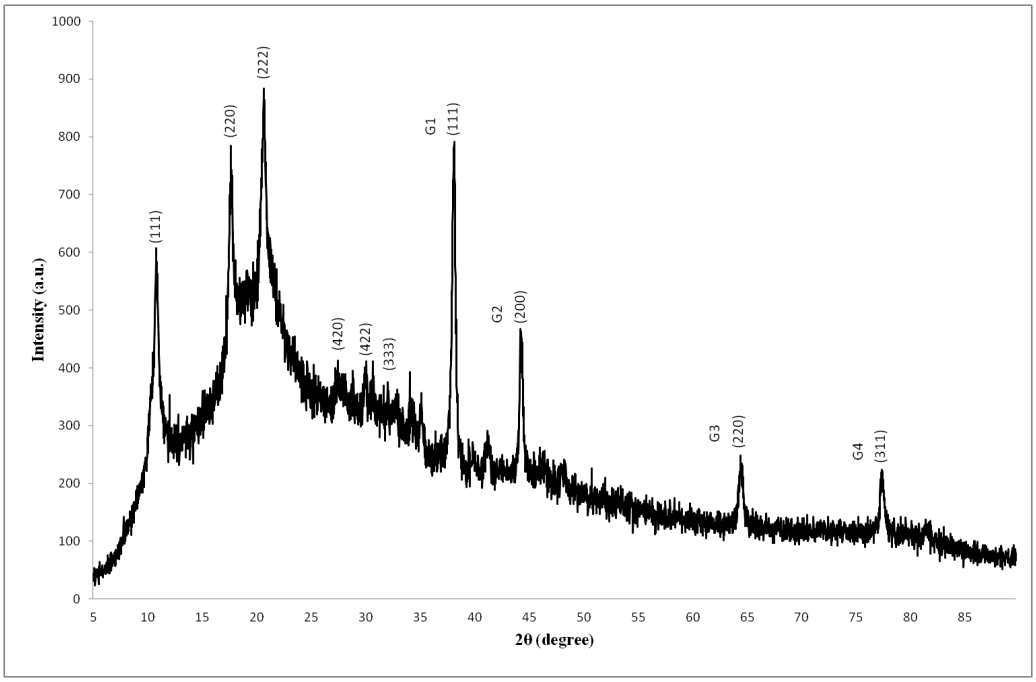

Figure 1. XRD pattern of [C_{60}]fullerene nanowhisker-gold nanoparticle composites

peared in the presence of 5 mg (13.2 mM) $NaBH_4$ dissolved in 10 ml distilled water. 1 mg [C_{60}]fullerene nanowhisker-gold nanoparticle composites was used as the catalyst for the 4-nitrophenol reduction. The absorbance was monitored at 2 min intervals to confirm the 4-nitrophenol reduction.

3. Results and Discussion

3.1 Characterization of [C_{60}]fullerene nanowhisker-gold nanoparticle composites

The crystal structure and crystallite size of the [C_{60}]fullerene nanowhisker-gold nanoparticle composites were examined by XRD. Figure 1 shows the XRD patterns of the [C_{60}]fullerene nanowhisker-gold nanoparticle composites. Peaks at 2θ = 10.82°, 17.68°, 20.72°, 27.53°, 30.13°, and 32.14° were due to the [C_{60}]fullerene nanowhiskers, and were assigned to the (111), (220), (222), (420), (422), and (333) planes, respectively. Peaks at 2θ = 38.20°, 44.33°, 64.61°, and 77.63° were due to the gold nanoparticles, and were assigned to the (111), (200), (220), and (311) planes, respectively. The crystallite size of the gold nanoparticles was calculated using the Scherrer equation:

$$D = \lambda K / \beta \cos \theta$$

where K is a shape factor taken as 0.9, λ is the wavelength of powder X-ray diffraction with Cu K_α radiation (λ=1.54178 Å), β is the full width at half maximum (FWHM), and 2θ is the angle between the incident and scattered X-rays. The Scherrer equation was used to calculate the crystallite size of the gold nanoparticles, as shown in Table 1. The mean crystallite size of the gold nanoparticles was 22.74 nm. Figure 2 shows the SEM image of the [C_{60}]fullerene nanowhisker-gold nanoparticle composites. The gold nanoparticles agglomerated on the [C_{60}]fullerene nanowhiskers, which are needle-like fibres. The many tiny crystals shown in Figure 2 are gold nanoparticles. The amount of gold nanoparticles loaded on the fullerene nanowhiskers was 0.25 mM. Figure 3 shows the Raman spectra of the nanocomposites. Raman shifts were observed for the peak of the [C_{60}]fullerene nanowhisker-gold nanoparticle composites, which showed squashing mode $H_g(1)$ at 271 cm^{-1}, breathing mode $A_g(1)$ at 494 cm^{-1}, and pentagonal pinch mode $A_g(2)$ at 1460 cm^{-1}.

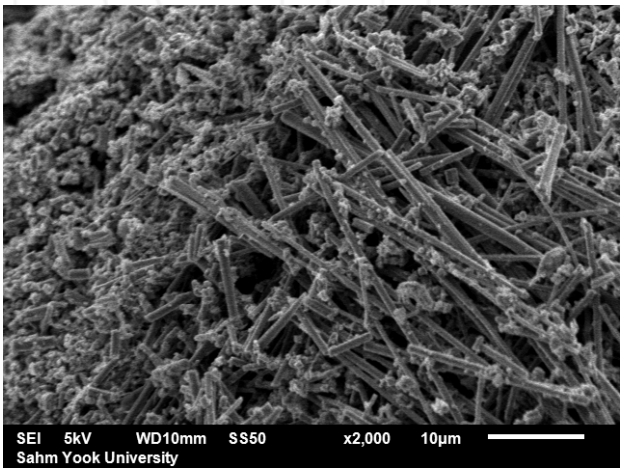

Figure 2. SEM image of [C_{60}]fullerene nanowhisker-gold nanoparticle composites

Peak	2-Theta	FWHM(B)	Crystallite size (nm)
G1	38.20	0.3545	24.87 nm
G2	44.33	0.4923	18.20 nm
G3	64.61	0.3545	27.87 nm
G4	77.63	0.5317	20.02 nm
Average			22.74 nm

Table 1. Crystallite size of gold nanoparticles, estimated using the Scherrer equation

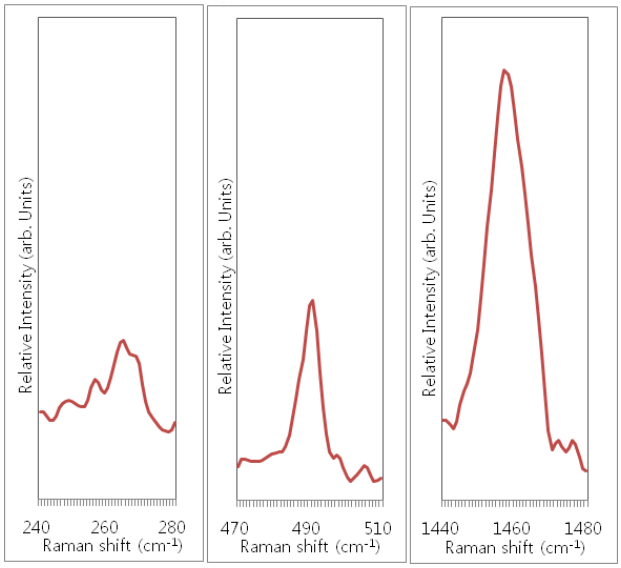

Figure 3. Raman spectra of [C_{60}]fullerene nanowhisker-gold nanoparticle composites

The Raman spectroscopy of the [C_{60}]fullerene nanowhisker-gold nanoparticle composites used a laser wavelength of 532 nm and a laser power density of 10 mW/mm^2.

From the Raman shift data, which showed a blue shift of $A_g(2)$ to 1460 cm^{-1}, we can confirm that the [C_{60}]fullerene nanowhiskers polymerized from [C_{60}]fullerene to form longer needle-like crystals.

Figure 4(a) and 4(b) show TEM images of the [C_{60}]fullerene nanowhisker-gold nanoparticle composites. Heat-treated [C_{60}]fullerene nanowhiskers collapsed and had a porous morphology, as seen from the TEM images shown in Figure 4(b) . As can be seen, the gold nanoparticles are located on the surface of the [C_{60}]fullerene nanowhiskers in the composites. The width of the composites is about 200 nm, and the size of the gold nanoparticles is 10-15 nm.

Figure 5 shows the solid-state ^{13}C-CP/ MAS NMR spectrum of the [C_{60}]fullerene nanowhisker-gold nanoparticle composites. The chemical shift observed at 143.60 ppm can be assigned to the sp^2 carbon, and the peak observed at 30.68 ppm to the sp^3 carbon. This means that polymerized intermolecular bonds of C_{60}-C_{60} may exist in the composites.

3.2 Catalytic and kinetic activity of [C_{60}]fullerene nanowhisker-gold nanoparticle composites for 4-nitrophenol reduction

Figure 6 shows the catalytic activity of the [C_{60}]fullerene nanowhisker-gold nanoparticle composites for the 4-nitrophenol reduction using $NaBH_4$. The UV-vis spectrum shows that the peak at 400 nm, related to the formation of 4-nitrophenolate ions under alkaline conditions after the addition of $NaBH_4$, was diminished. A new peak at 300 nm simultaneously appeared due to 4-aminophenol production in the presence of the [C_{60}]fullerene nanowhisker-gold nanoparticle composites. In Figure 6(a), without the composites, the peak due to the 4-nitrophenolate ion remained unaltered for 40 min, showing the inability of $NaBH_4$ to reduce the 4-nitrophenolate ion to 4-aminophenol, even though it is known to be a strong reducing agent. Therefore, the [C_{60}]fullerene nanowhisker-gold nanoparticle composites operated as a catalyst for the 4-nitrophenol, as shown in Figure 6(b). Figure 7 shows the kinetic activity in the reduction of 4-nitrophenol using the composites as a catalyst. In previous studies, the Langmuir-Hinshelwood model has been applied to study the kinetics of 4-nitrophenol reduction [37-40]. The kinetic equation can be written as follows: $\ln(C/C_0) = -\kappa t$, where C_0 is the initial concentration, C is the concentration at time t, and κ is the rate constant. The reduction of 4-nitrophenol obeyed a pseudo-first-order rate law. The [C_{60}]fullerene nanowhisker-gold nanoparticle composites, as compared to the other system, exhibited similar catalytic efficiency [33,35].

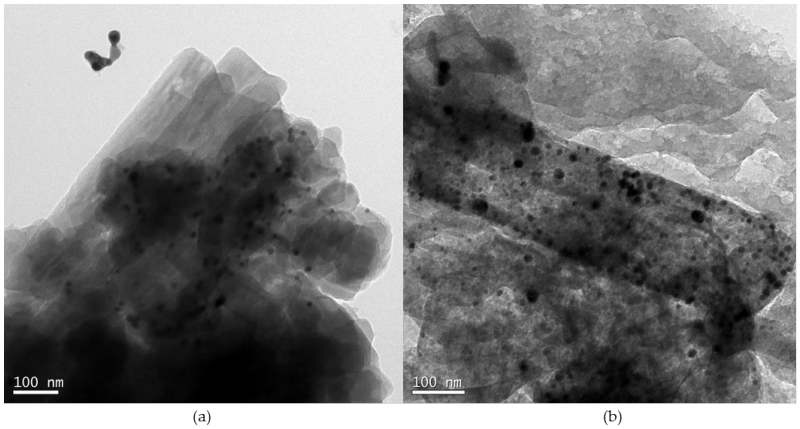

(a) (b)

Figure 4. TEM images of (a) unheated and (b) heated [C_{60}]fullerene nanowhisker-gold nanoparticle composites

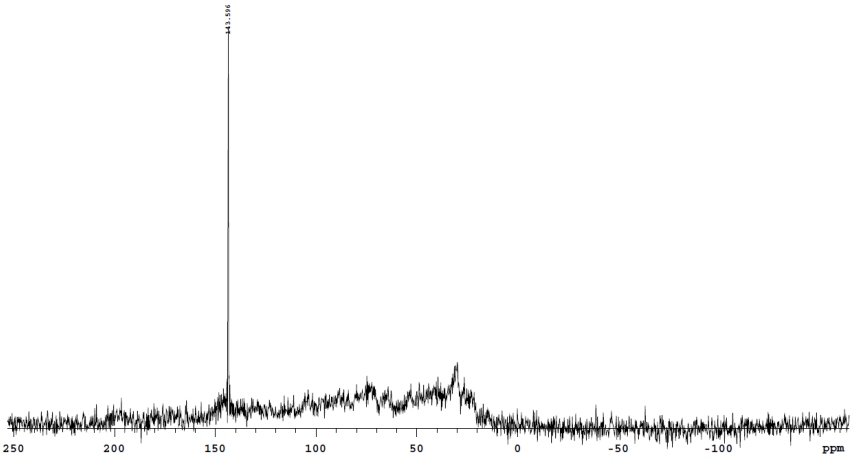

Figure 5. Solid-state ^{13}C-CP/MAS NMR spectrum of [C_{60}]fullerene nanowhisker-gold nanoparticle composites

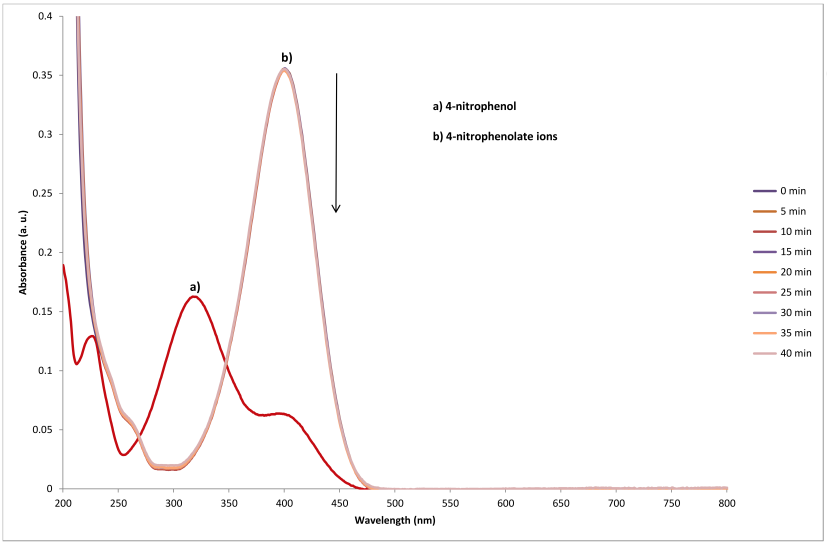

(a)

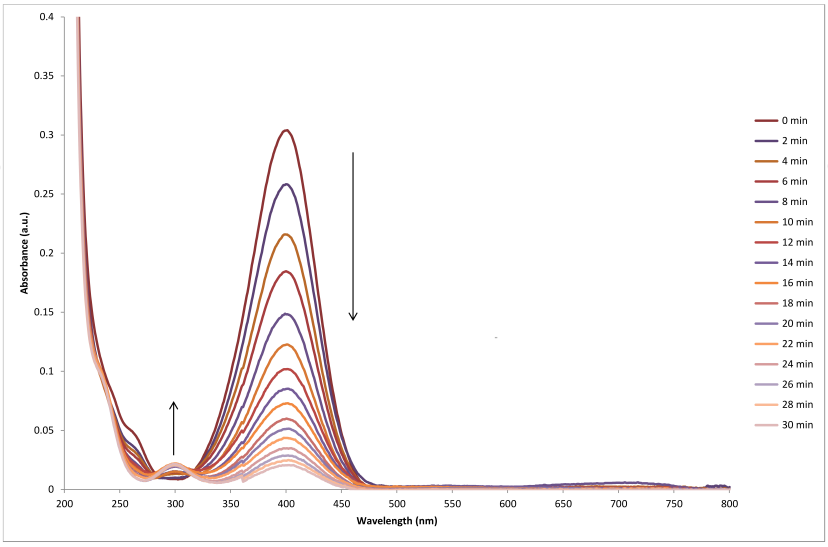

(b)

Figure 6. UV-vis spectra of 4-nitrophenol reduction with $NaBH_4$ (a) in the absence of and (b) in the presence of [C_{60}]fullerene nanowhisker-gold nanoparticle composites

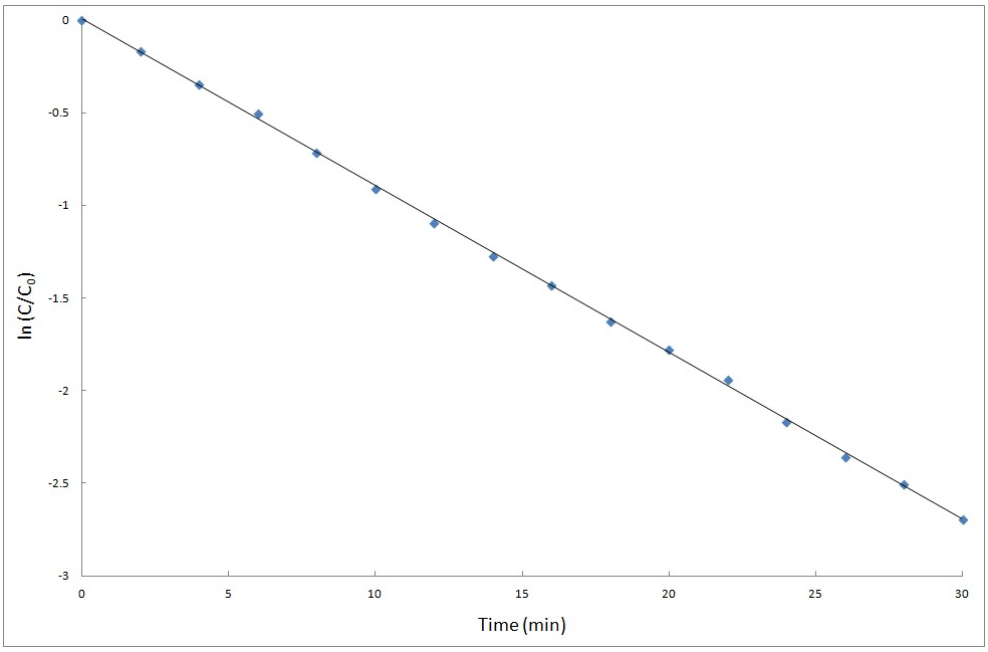

Figure 7. Kinetics of reduction of 4-nitrophenol using [C_{60}]fullerene nanowhisker-gold nanoparticle composites

4. Conclusions

[C_{60}]fullerene nanowhisker-gold nanoparticle composites were synthesized from gold nanoparticle solution, [C_{60}]fullerene-saturated toluene, and isopropyl alcohol solution, using the LLIP method. The composites were characterized by XRD, Raman spectroscopy, SEM, TEM, and solid-state ^{13}C-CP/MAS NMR spectroscopy. The reduction of 4-nitropheqnol when applied with $NaBH_4$ resulted in good catalytic activity of the composites using UV-vis spectroscopy. The catalytic activity of the 4-nitrophenol reduction with the [C_{60}]fullerene nanowhisker-gold nanoparticle composites showed pseudo-first-order reaction kinetics.

5. Acknowledgements

This study was supported by research funding from Sahmyook University, South Korea.

6. References

[1] Kroto H W, Health J R, O'Brein S C, Curl R F, Smalley R E (1985) C_{60}:buckminsterfullerene. Nature 318:162-163.

[2] Miyazawa K (2015) Synthesis of fullerene nanowhiskers using the liquid-liquid interfacial precipitation method and their mechanical, electrical and superconducting properties. Science and Technology of Advanced Materials 16(1): 013502-013511.

[3] Miyazawa K (2011) Fullerene Nanowhiskers. Pan Stanford Publishing Pte. Ltd. pp. 209.

[4] Miyazawa K, Kuwasaki Y, Obayashi A, Kuwabara M (2002) C_{60} nanowhiskers formed by liquid-liquid interfacial precipitation method. Journal of Materials Research 17(1): 83-88.

[5] Osonoe K, Kano R, Miyazawa K, Tachibana M (2014) Synthesis of C_{70} two-dimensional nanosheets by liquid–liquid interfacial precipitation method. Journal of Crystal Growth 401: 458-461.

[6] Wakahara T, Sathish M, Miyazawa K, Hu C, Tateyama Y, Nemoto Y, Sasaki T, Ito O (2009) Preparation and optical properties of fullerene/ferrocene hydrid hexagonal nanosheets and large-scale production of fullerene hexagonal nanosheets. Journal of the American Chemical Society 131(29): 9940-9944.

[7] Shrestha L K, Sathish M, Hill J P, Miyazawa K, Tsuruoka T, Sanchez-Ballester N M, Honma I, Ji Q, Ariga K (2013) Alcohol-induced decomposition of Olmstead's crystalline Ag(I)-fullerene heteronanostructure yields 'bucky cubes'. Journal of Materials Chemistry C 2013(6): 1174-1181.

[8] Shrestha L K, Hill J P, Tsuruoka T, Miyazawa K, Ariga K (2013) Surfactant-assisted assembly of fullerene (C_{60}) nanorods and nanotubes formed at liquid-liquid interface. Langmuir 29(24): 7195-7202.

[9] Shrestha L K, Ji Q, Mori T, Miyazawa K, Yamauchi Y, Hill J P, Ariga K (2013) Fullerene nanoarchitectonics: from zero to higher dimensions. Chemistry – An Asian Journal 8(8): 1662-1679.

[10] Shrestha L K, Yamauchi Y, Hill J P, Miyazawa K, Ariga K (2013) Fullerene crystals with bimodal pore architectures consisting of macropores and mesopores. Journal of the American Chemical Society 135(2): 586-589.

[11] Shrestha L K, Hill J P, Miyazawa K, Ariga K (2012) Mixing antisolvents induced modulation in the

morphology of crystalline C_{60}. Journal of Nanoscience and Nanotechnology 12(8): 6380-6384.

[12] Sathish M, Miyazawa K (2007) Size-tunable hexagonal fullerene (C_{60}) nanosheets at liquid-liquid interface. Journal of the American Chemical Society 129(45): 13816-13817.

[13] Miyazawa K, Kuwasaki Y, Hamamoto K, Nagata S, Obayashi A, Kuwabara M (2003) Structural characterization of C_{60} nanowhiskers formed by liquid/liquid interfacial precipitation method. Surface and Interface Analysis 35(1): 117-120.

[14] Wakahara T, Sathish M, Miyazawa K, Ito O (2015) Electrochemical characterization of catalytic activities of C_{60} nanowhiskers to oxygen in aqueous solution. Fullerenes, Nanotubes and Carbon Nanostructures 23(6): 509-512.

[15] Sathish M, Miyazawa K, Sasaki T (2007) Nanoporous fullerene nanowhiskers. Chemistry of Materials 19(10): 2398-2400.

[16] Miyazawa K, Hotta K (2010) The effect of solvent ratio and water on the growth of C_{60} nanowhiskers. Journal of Crystal Growth 312(19): 2764-2770.

[17] Ringor C L, Miyazawa K (2008) Synthesis of C_{60} nanotubes by liquid–liquid interfacial precipitation method: Influence of solvent ratio, growth temperature, and light illumination. Diamond and Related Materials 17(4-5): 529-534.

[18] Tachibana M, Kobayashi K, Uchida T, Kojima K, Tanimura M, Miyazawa K (2003) Photo-assisted growth and polymerization of C_{60} 'nano'whiskers. Chemical Physics Letters 374(3-4): 279-285.

[19] Miyazawa K, Hotta K (2011) The effect of water on the stability of C_{60} fullerene nanowhiskers. Journal of Nanoparticle Research 13(11): 5739-5747.

[20] Hotta K, Miyazawa K (2008) Growth rate measurement of C_{60} fullerene nanowhiskers. Nano 3(5): 355.

[21] Sathish M, Miyazawa K (2012) Synthesis and characterization of fullerene nanowhiskers by liquid-liquid interfacial precipitation: influence of C_{60} solubility. Molecules 17: 3858-3865.

[22] Kato R, Miyazawa K (2012) Raman laser polymerization of C_{60} nanowhiskers. Journal of Nanotechnology 2012: 101243-101248.

[23] Miyazawa K, Minato J, Fujino M, Suga T (2006) Structural investigation of heat-treated fullerene nanotubes and nanowiskers. Diamond and Related Materials 15(4-8): 1143-1146.

[24] Asaka K, Kato R, Miyazawa K, Kizuka T (2006) Buckling of C_{60} nanowhiskers. Applied Physics Letters 89(7): 017912.

[25] Rao A M, Zhou P, Wang K A, Hager G T, Holden J M, Wang Y, Lee W T, Bi X X, Ecklund P C, Cornett D S (1993) Photoinduced polymerization of solid C_{60} films. Science 259(5097): 955-957.

[26] Lee H J, Hong S K, Kim J M, Ko W B (2011) Synthesis of gold nanoparticles using pluronic® F127NF under microwave irradiation and catalytic effects. Journal of Nanoscience and Nanotechnology 11(1): 734-737.

[27] Miyazawa K (2011) Fullerene Nanowhiskers. Pan Stanford Publishing Pte. Ltd., pp. 242.

[28] Qiu L, Peng Y, Liu B, Lin B, Peng Yu, J. Malik M, Yan F (2012) Polypyrrole nanotube-supported gold nanoparticles: An efficient electrocatalyst for oxygen reduction and catalytic reduction of 4-nitrophenol. Applied Catalysis A: General 413-414(31): 230-237.

[29] Li H, Jo J K, Zhang L, Ha C S, Suh H and Kim I L (2010) A General and Efficient Route to Fabricate Carbon Nanotube-Metal Nanoparticles and Carbon Nanotube-Inorganic Oxides Hybrids. Advanced Functional Materials 20(22): 3864-3873.

[30] Zhang M, Liu L, Wu C, Fu G, Zhao H, He B (2007) Synthesis, characterization and application of well-defined environmentally responsive polymer brushes on the surface of colloid particles. Polymer 48(7): 1989-1997.

[31] Jana S, Ghosh S K, Nath S, Pande S, Praharaj S, Panigrahi S, Basu S, Endo T, Pal T (2006) Synthesis of silver nanoshell-coated cationic polystyrene beads: A solid phase catalyst for the reduction of 4-nitrophenol. Applied Catalysis A: General 313(1): 41-48.

[32] Nemeth T, Jankovics P, Nemeth-palotas J, Koszegi-Szalai H (2008) Determination of paracetamol and its main impurity 4-aminophenol in analgesic preparations by micellar electrokinetic chromatography. Journal of Pharmaceutical and Biomedical Analysis 47: 746-749.

[33] Wang Z, Xu C, Li X, Liu Z (2015) In situ green synthesis of Ag nanoparticles on tea polyphenols-modified grapheme and their catalytic reduction activity of 4-nitrophenol. Colloids and Surfaces A: Physicochem. Eng. Aspects 485: 102-110.

[34] Xia J, He G, Zhang L, Sun X, Wang X (2016) Hydrogenation of nitrophenols catalyzed by carbon black-supported nickel nanoparticles under mild conditions. Applied Catalysis B: Environmental 180: 408-415.

[35] Zhao P, Feng X, Huang D, Yang G, Astruc D (2015) Basic concepts and recent advances in nitrophenol reduction by gold-and other transition metal nanoparticles. Coordination Chemistry Reviews 287: 114-136.

[36] Premkumar T, Lee K, Geckeler K (2011) Shape-tailoring and catalytic function of anisotropic gold nanostructures. Nanoscale Research Letters 6: 547.

[37] Feng J, Su L, Ma Y, Ren C, Guo Q, Chen X (2013) $CuFe_2O4$ magnetic nanoparticles: A simple and

efficient catalyst for the reduction of nitrophenol. Chemical Engineering Journal 221: 16-24.

[38] Borah B J, Bharali P (2014) Surfactant-free synthesis of CuNi nanocrystals and their application for catalytic reduction of 4-nitrophenol. Journal of Molecular Catalysis A: Chemical 390: 29-36.

[39] Wunder S, Polzer F, Lu Y, Mei Y, Ballauff M (2010) Kinetic Analysis of Catalytic Reduction of 4-Nitrophenol by Metallic Nanoparticles Immobilized in Spherical Polyelectrolyte Brushes. The Journal of Physical Chemistry C 114(19): 8814-8820.

[40] Taghavi F, Falamaki C, Shabanov A, Bayrami L, Roumianfar A (2011) Kinetic study of the hydrogenation of p-nitrophenol to p-aminophenol over micro-aggregates of nano-Ni2B catalyst particles. Applied Catalysis A: General 407(1-2): 173-180.